Original research article

Perturbation of dispersive optical solitons with Schrödinger–Hirota equation with Kerr law and spatio-temporal dispersion

Neslihan Ozdemir [a], Aydin Secer [b,c,*], Muslum Ozisik [b], Mustafa Bayram [c]

[a] *Department of Software Engineering, Istanbul Gelisim University, Istanbul, Turkey*
[b] *Department of Mathematical Engineering, Yildiz Technical University, Istanbul, Turkey*
[c] *Biruni University, Department of Computer Engineering, Istanbul, Turkey*

ARTICLE INFO

ABSTRACT

Objective: The principal purpose of this paper is to examine the perturbed Schrödinger–Hirota equation with the effect of spatio-temporal dispersion and Kerr law nonlinearity which governs the propagation of dispersive pulses in optical fibers by proposing and using a direct algebraic form of the enhanced modified extended tanh expansion method for the first time. Our aim is not only restricted to obtaining different and more soliton solutions by proposed method for the first time in this study, but also includes examining the effect of the coefficients of self-steepening and nonlinear dispersion terms to the soliton propagation in the investigated problem.

Methodology: Utilizing a traveling wave transformation, the perturbed Schrödinger–Hirota equation with the effect of spatio-temporal dispersion and Kerr law nonlinearity can be transformed into an nonlinear ordinary differential equation (NODE). Then, the NODE is convert into a set of algebraic equations by taking account into the Riccati differential equation. Solving the set of algebraic equations, we acquire the analytical soliton solutions of the perturbed Schrödinger–Hirota equation with the effect of spatio-temporal dispersion and Kerr law nonlinearity. In the proposed method, the modified extended tanh function method is enhanced by presenting more solutions of Riccati differential equations with the direct algebraic form, is utilized.

Results: The more solutions have been established to the literature with new significant physical properties of the perturbed Schrödinger–Hirota equation with the effect of spatio-temporal dispersion and Kerr law nonlinearity. We indicated that the presented method are effective, easily computable, and reliable in solving such nonlinear problems. Moreover, we demonstrate the dynamical behaviors and physical significance of some soliton solutions at appropriate values of parameters.

Originality: A variety of soliton solutions to the perturbed Schrödinger–Hirota equation with Kerr law non-linearity by the direct algebraic form of enhanced modified extended tanh expansion method have been acquired. These solutions are dark–bright, trigonometric, hyperbolic, periodic, and singular soliton solutions. 3D, contour and 2D plots of some obtained solutions have been demonstrated to interpret the physical meaning of the equation. For some parameter values in the equation, the behavior of soliton solutions has been examined. The constraint conditions are established to confirm the existence of valid solutions. The obtained results can be effective in interpreting the physical meaning of this nonlinear system. We have seen that the proposed direct algebraic form of the enhanced modified extended tanh expansion method

* Corresponding author at: Department of Mathematical Engineering, Yildiz Technical University, Istanbul, Turkey.
E-mail addresses: neozdemir@gelisim.edu.tr (N. Ozdemir), asecer@yildiz.edu.tr (A. Secer), ozisik@yildiz.edu.tr (M. Ozisik), mustafabayram@biruni.edu.tr (M. Bayram).

is a powerful mathematical technique which can be utilized to acquire the analytical solutions to different complex nonlinear mathematical models.

1. Introduction

Nonlinear evolution equations (NLEEs) are applied to identify a variety of the physical phenomena in the several branches of science like optical fibers, plasma physics, biology, chemistry, physics. In recent years, soliton solutions and their features have been particularly examined in different fields such as fluid dynamics, optical fibers, birefringent fibers, ocean engineering, etc in [1–3]. Acquiring the analytical and soliton solutions of NLEEs has importance since they have strong practical importance in various areas. So, a variety of the efficient method have been improved to achieve the analytical and soliton solutions of NLEEs such as the Jacobi elliptic function approach [4], the extended auxiliary equation approach [5], the Lie symmetry analysis [6,7], the unified Riccati equation [8], the extended trial function algorithm [9], the Kudryashov's method [10], the extended Kudryashov's method [11], the semi-inverse variational principle [12,13], the Sardar subequation and the new Kudryashov methods [14], the modified extended tanh expansion method [15], the extended sinh-Gordon equation expansion method [16,17], the $\frac{G'}{G^2}$ expansion function method [16,18,19], the sine–cosine method [19], the $\frac{G'}{G}$-expansion method [20,21], the exp-function method [21,22], Riccati–Bernoulli sub-ODE method [23,24], the Kudryashov-expansion method [25,26], the rational sine–cosine method [26], the modified simple equation method [27–30], the trial equation method [29,30], the modified tanh–coth method [31], the asymmetric method [32], the F-expansion scheme [33], the functional variable method and first integral approach [34], He's semi-inverse variational principle [35].

The dynamics of soliton propagation through optical fibers is governed by the nonlinear evolution equation. As is known, in some cases, one of the methods used to prevent the low group velocity dispersion (GVD) in optical fibers is the addition of third-order dispersion (3OD), which causes dispersive optical solitons. The Schrödinger–Hirota equation (SHE) is one of the important models in which this type of modeling [36]. SHE describes the real-world models in nonlinear optics and dispersive optical fibers. The equation and its solutions, which ensure interpret phenomena, have attracted a lot of attention recently, thanks to applications in a wide variety of fields, particularly in optical communication systems.

In order to model the optical propagation in fiber in presence of 3OD is given by nonlinear Schrödinger equation as [37]

$$i\frac{\partial h}{\partial t} + \frac{1}{2}\frac{\partial^2 h}{\partial x^2} + |h|^2 h = -i\alpha\frac{\partial^3 h}{\partial x^3}, \tag{1}$$

in which $h = h(x, t)$ is solution profile and, $\frac{\partial h}{\partial t}$ is the linear temporal evolution term, $\frac{\partial^2 h}{\partial x^2}$ is the GVD term, $|h|^2$ is Kerr law nonlinearity term, $\frac{\partial^3 h}{\partial x^3}$ is the 3OD and, α is the coefficient of 3OD term.

Using the Lie transform [37,38]:

$$\vartheta = h - 3i\alpha\left[h_x + 2h\int_{-\infty}^{x}|h(\xi)|^2 d\xi\right]. \tag{2}$$

Eq. (1) converts to the following equation:

$$i\vartheta_t + \frac{1}{2}\vartheta_{xx} + |\vartheta|^2\vartheta + i\alpha\left(\vartheta_{xxx} + 6|\vartheta|^2\vartheta_x\right) = 0, \tag{3}$$

in which $\vartheta = \vartheta(x, t)$. If the nonlinear terms are omitted, Eq. (3) is called the nonlinear Schrödinger equation (NLSE) with Kerr law nonlinearity and it can be given in the following general form by organizing the coefficient with arbitrary numbers:

$$i\frac{\partial\vartheta}{\partial t} + \lambda_1\frac{\partial^2\vartheta}{\partial x^2} + \lambda_3|\vartheta|^2\vartheta + i\left(\alpha\frac{\partial^3 h}{\partial x^3} + \beta|\vartheta|^2\frac{\partial\vartheta}{\partial x}\right) = 0, \tag{4}$$

in which λ_1, λ_3 and, β are any real non-zero free parameters. λ_1 and β are the coefficients of the GVD and the nonlinear dispersion term, respectively. Because of the relation of the GVD and ill-pose of the model, in order to make the model well-pose an additional term which is called spatio-temporal dispersion (STD) is added [36,39]. So, Eq. (4) becomes:

$$i\frac{\partial\vartheta}{\partial t} + \lambda_1\frac{\partial^2\vartheta}{\partial x^2} + \lambda_2\frac{\partial^2\vartheta}{\partial x\partial t} + \lambda_3|\vartheta|^2\vartheta + i\left(\alpha\frac{\partial^3\vartheta}{\partial x^3} + \beta|\vartheta|^2\frac{\partial\vartheta}{\partial x}\right) = 0, \tag{5}$$

in which λ_2 is the coefficient of the STD term. When the perturbation term is taken into account, Eq. (5) turns into the perturbed Schrödinger–Hirota equation with the effect of spatio-temporal dispersion and Kerr law nonlinearity (pSHE-STD-KL), which we have discussed in the article.

In this paper, we carried out optical soliton solutions of the perturbed Schrödinger–Hirota equation with the effect of pSHE-STD-KL which models the propagation of dispersive pulses in optical fibers is described by [36,40]:

$$i\frac{\partial\vartheta}{\partial t} + \lambda_1\frac{\partial^2\vartheta}{\partial x^2} + \lambda_2\frac{\partial^2\vartheta}{\partial x\partial t} + \lambda_3|\vartheta|^2\vartheta + i\left(\alpha\frac{\partial^3\vartheta}{\partial x^3} + \beta|\vartheta|^2\frac{\partial\vartheta}{\partial x}\right) = i\left(a\frac{\partial\vartheta}{\partial x} + b\frac{\partial(|\vartheta|^2\vartheta)}{\partial x} + c\frac{\partial|\vartheta|^2}{\partial x}\vartheta\right), \tag{6}$$

in which λ_1, λ_2 and α are the coefficients of the GVD, the STD and the 3OD terms, respectively. The parameters λ_3 and β are the coefficients of nonlinear dispersion term. The coefficients $a, b,$ and c stand for the inter-modal dispersion (IMD), the self-steepening,

and the nonlinear dispersion, respectively. The complex function $\vartheta = \vartheta(x,t)$ is the soliton profile, $i = \sqrt{-1}$, and Eq. (6) is expressed as generalization of the NLSE. Besides, in Eq. (6), the right-hand side symbolizes the perturbation.

In this paper, we aim to introduce the direct algebraic enhanced modified extended tanh expansion method to examine analytical and soliton solutions of the pSHE-STD-KL equation. Up to now, the proposed method has not been implemented to any nonlinear partial differential equations in the literature as presented. To date, pSHE-STD-KL has been examined to get a variety of solutions by few methods. These methods are the improved Sardar sub-equation method [36], the auxiliary equation and the modified auxiliary equation method [41], the Q-deformed hyperbolic functions method and Q-deformed trigonometric functions method [42], the modified Khater method [43]. In [44], numerical solutions for the dispersive optical soliton solutions of the pSHE-STD-KL were obtained via the improved Adomian decomposition method.

This research paper is parted into the following sections. In Section 2, the mathematical analysis of the pSHE-STD-KL is constituted. In a detailed manner, the direct algebraic enhanced modified extended tanh expansion is proposed in Section 3. The method is employed to the pSHE-STD-KL to acquire various soliton solutions in Section 4. The obtained results are reported in Section 5. In the last section, conclusion part is presented.

2. Description of the proposed method

In this section, we introduce a different version of direct algebraic form of modified extended tanh expansion method with more solution sets. In the generalized modified extended tanh expansion method [45], the following Riccati equation is utilized:

$$\Psi'(\eta) = w + \Psi^2(\eta), \tag{7}$$

and in the literature, generally Eq. (7) is given with the solutions $\Psi_1^+(\eta), \Psi_2^+(\eta), \Psi_8^+(\eta), \Psi_9^+(\eta)$ and $\Psi_{15}^+(\eta)$ in Situation-1 to Situation-3.

Consider the following nonlinear partial differential equation:

$$P(\vartheta, \vartheta_x, \vartheta_t, \vartheta_{tt}, \vartheta_{xt}, \vartheta_{xx}, \ldots) = 0, \tag{8}$$

in which $\vartheta = \vartheta(x,t)$ and, subscript x, t denotes the partial derivatives of $\vartheta(x,t)$ with respect to x and t.

In order to transform Eq. (8) to NODE, we apply the following new transformation:

$$\vartheta(x,t) = \psi(\eta), \quad \eta = x - \upsilon t \tag{9}$$

where υ is the wave speed of the soliton. Inserting Eq. (9) into Eq. (8), we get the following NODE in the following form:

$$Q(\psi(\eta), \psi'(\eta), \psi''(\eta), \ldots) = 0. \tag{10}$$

The solution of Eq. (10) is proposed as follow:

$$\psi(\eta) = A_0 + \sum_{m=1}^{M} A_m \Psi^m(\eta) + \sum_{m=1}^{M} \frac{B_m}{\Psi^m(\eta)}. \tag{11}$$

In Eq. (11), $A_0, A_m, B_m, (m = 1, 2, \ldots, M)$ are unknown coefficients to be calculated and M is the balancing constant which is acquired by the balancing rule in Eq. (10), also A_m, B_m should not be zero, simultaneously.

In Eq. (11), the $\Psi(\eta)$ function admits the following formula:

$$\Psi'(\eta) = \ln(K)\left(w \mp \Psi^2(\eta) \right), 0 < K \neq 1, \tag{12}$$

in which w is real value. We can write some solutions of Eq. (12) as follow:

Situation-1:

$$\Psi_1^{\mp}(\eta) = \pm\sqrt{\pm w} \tanh_K\left(\sqrt{\pm w}\,(\eta + \eta_0) \right),$$

$$\Psi_2^{\mp}(\eta) = \pm\sqrt{\pm w} \coth_K\left(\sqrt{\pm w}\,(\eta + \eta_0) \right),$$

$$\Psi_3^{\mp}(\eta) = \pm\sqrt{\pm w}\left(\tanh_K\left(2\sqrt{\pm w}\,(\eta + \eta_0) \right) \mp i\gamma \, sech_K\left(2\sqrt{\pm w}\,(\eta + \eta_0) \right) \right),$$

$$\Psi_4^{\mp}(\eta) = \mp\frac{\left(w - \sqrt{\pm w} \tanh_K\left(\sqrt{\pm w}\,(\eta + \eta_0) \right) \right)}{\left(1 \mp \sqrt{\pm w} \tanh_K\left(\sqrt{\pm w}\,(\eta + \eta_0) \right) \right)},$$

$$\Psi_5^{\mp}(\eta) = \mp\frac{\sqrt{\pm w}\left(5 - 4\cosh_K\left(2\sqrt{\pm w}\,(\eta + \eta_0) \right) \right)}{\left(3 + 4\sinh_K\left(2\sqrt{\pm w}\,(\eta + \eta_0) \right) \right)},$$

$$\Psi_6^{\mp}(\eta) = \mp\frac{\gamma\sqrt{\pm w\,(\rho^2 + \sigma^2)} - \rho\sqrt{\pm w}\cosh_K\left(2\sqrt{\pm w}\,(\eta + \eta_0) \right)}{\rho\sinh_K\left(2\sqrt{\pm w}\,(\eta + \eta_0) \right) + \beta},$$

$$\Psi_7^{\mp}(\eta) = \gamma\sqrt{\pm w}\left[1 - \frac{2\rho}{\rho + \cosh_K\left(2\sqrt{\pm w}\left(\eta + \eta_0\right)\right) \pm \gamma\sinh_K\left(2\sqrt{\pm w}\left(\eta + \eta_0\right)\right)}\right],$$

in which

$$\sinh_K\left(\Omega\eta\right) = \frac{K^{\Omega\eta} - K^{-\Omega\eta}}{2},$$

$$\cosh_K\left(\Omega\eta\right) = \frac{K^{\Omega\eta} + K^{-\Omega\eta}}{2},$$

$$\tanh_K\left(\Omega\eta\right) = \frac{K^{\Omega\eta} - K^{-\Omega\eta}}{K^{\Omega\eta} + K^{-\Omega\eta}},$$

$$\coth_K\left(\Omega\eta\right) = \frac{K^{\Omega\eta} + K^{\Omega\eta}}{K^{\Omega\eta} - K^{-\Omega\eta}},$$

$$sech_K\left(\Omega\eta\right) = \frac{2}{K^{\Omega\eta} + K^{-\Omega\eta}}.$$

Situation-2:

$$\Psi_8^{\mp}(\eta) = \mp\sqrt{\mp w}\tan_K\left(\sqrt{\mp w}\left(\eta + \eta_0\right)\right),$$

$$\Psi_9^{\mp}(\eta) = \pm\sqrt{\mp w}\cot_K\left(\sqrt{\mp w}\left(\eta + \eta_0\right)\right),$$

$$\Psi_{10}^{\mp}(\eta) = \mp\sqrt{\mp w}\left(\tan_K\left(2\sqrt{\mp w}\left(\eta + \eta_0\right)\right) \mp \sec_K\left(2\sqrt{\mp w}\left(\eta + \eta_0\right)\right)\right),$$

$$\Psi_{11}^{\mp}(\eta) = \pm\frac{\sqrt{\mp w}\left(1 - \tan_K\left(\sqrt{\mp w}\left(\eta + \eta_0\right)\right)\right)}{\left(1 + \tan_K\left(\sqrt{\mp w}\left(\eta + \eta_0\right)\right)\right)},$$

$$\Psi_{12}^{\mp}(\eta) = \mp\frac{\sqrt{\mp w}\left(4 - 5\cos_K\left(2\sqrt{\mp w}\left(\eta + \eta_0\right)\right)\right)}{\left(3 + 5\sin_K\left(2\sqrt{\mp w}\left(\eta + \eta_0\right)\right)\right)},$$

$$\Psi_{13}^{\mp}(\eta) = \mp\frac{\gamma\sqrt{\mp w\left(\rho^2 - \sigma^2\right)} - \rho\sqrt{\mp w}\cos_K\left(2\sqrt{\mp w}\left(\eta + \eta_0\right)\right)}{\rho\sin_K\left(2\sqrt{\mp w}\left(\eta + \eta_0\right)\right) + \sigma},$$

$$\Psi_{14}^{\mp}(\xi) = i\gamma\sqrt{\mp w}\left[1 - \frac{2\rho}{\rho + \cos_K\left(2\sqrt{\mp w}\left(\eta + \eta_0\right)\right) \pm i\gamma\sin_K\left(2\sqrt{\mp w}\left(\eta + \eta_0\right)\right)}\right],$$

in which

$$\sin_K\left(\Omega\eta\right) = -i\frac{K^{i\Omega\eta} - K^{-i\Omega\eta}}{2},$$

$$\cos_K\left(\Omega\eta\right) = \frac{K^{i\Omega\eta} + K^{-i\Omega\eta}}{2},$$

$$\tan_K\left(\Omega\eta\right) = -i\frac{K^{i\Omega\eta} - K^{-i\Omega\eta}}{K^{i\Omega\eta} + K^{-i\Omega\eta}},$$

$$\cot_K\left(\Omega\eta\right) = i\frac{K^{i\Omega\eta} + K^{-i\Omega\eta}}{K^{i\Omega\eta} - K^{-i\Omega\eta}},$$

$$sec_K\left(\Omega\eta\right) = \frac{2}{K^{i\Omega\eta} + K^{-i\Omega\eta}}.$$

Situation-3: If $w = 0$, then

$$\Psi_{15}^{\mp}(\eta) = \pm\frac{1}{ln(K)(\eta + \eta_0)},$$

in which $\Omega = \sqrt{\mp w}$, $\gamma = \mp 1$, ρ, σ, η_0 and w are any real non-zero free parameter.

Remark 1. In Situation-1 to Situation-2, for $\sqrt{w}$, w is positive, for $\sqrt{w}$, w is negative.

Remark 2. In the presented method, we utilize a direct algebraic form of enhanced modified extended expansion method in [46].

Remark 3. In this paper, we will use Eq. (12) in the following form:

$$\Psi'(\eta) - ln(K)(w - \Psi^2(\eta)) = 0.$$

3. Application

Consider the next wave transformations to acquire analytical traveling wave solutions of Eq. (6),

$$\vartheta(x,t) = \psi(\eta)e^{i\theta}, \quad \eta = p(x - vt), \ \theta = -kx + \omega t + \varrho_0, \tag{13}$$

in which v is the soliton velocity, θ, k, ω and ϱ_0 are the phase component, the soliton frequency, the soliton wave number, and the phase constant, respectively. Inserting Eq. (13) into Eq. (6) and dividing into real and imaginary parts yields a pair of relations. The real part and imaginary part are acquired as follows, respectively:

$$\frac{(-bk + \beta k + \lambda_3)}{3\alpha k\, p^2 - p^2 v \lambda_2 + p^2 \lambda_1}\psi^3 + \frac{(-\alpha\, k^3 - k^2 \lambda_1 + k\omega\lambda_2 - ak - \omega)\,\psi}{3\alpha k\, p^2 - p^2 v \lambda_2 + p^2 \lambda_1} + \psi'' = 0, \tag{14}$$

$$\frac{\left(\frac{1}{3}\beta p - bp - \frac{2}{3}cp\right)}{\alpha\, p^3}\psi^3 + \frac{(-3\alpha\, k^2 p + kpv\lambda_2 - 2kp\lambda_1 + \omega p\lambda_2 - ap - pv)\,\psi}{\alpha\, p^3} + \psi'' = 0, \tag{15}$$

where $\psi = \psi(\eta)$, $\psi' = \frac{d\psi(\eta)}{d\eta}$ and after using the homogeneous balance principle between Eq. (14) and, Eq. (15), we acquire the following constraint conditions:

$$\lambda_3 = \frac{6\alpha bk + 6\alpha ck - 3bv\lambda_2 + \beta v\lambda_2 - 2cv\lambda_2 + 3b\lambda_1 - \beta\lambda_1 + 2c\lambda_1}{3\alpha}, \tag{16}$$

$$a = \frac{-8\alpha^2 k^3 + 6\left(v\lambda_2 - \frac{4\lambda_1}{3}\right)\alpha\, k^2 + \left(-v^2\lambda_2^2 + (2\alpha\omega + 3v\lambda_1)\,\lambda_2 - 3\alpha v - 2\lambda_1^2\right)k - \omega v\lambda_2^2 + (\omega\lambda_1 + v^2)\,\lambda_2 - v\lambda_1 + \alpha\omega}{2\alpha k - v\lambda_2 + \lambda_1}. \tag{17}$$

Under these constraint conditions, Eq. (15) can be taken into account NODE form of Eq. (6) and, with the assistance of the homogeneous balance rule by taking the terms ψ'' and ψ^3 in Eq. (15), $M = 1$ is acquired. So, Eq. (11) transforms into the following form:

$$\psi(\eta) = A_0 + A_1\Psi(\eta) + \frac{B_1}{\Psi(\eta)}. \tag{18}$$

Substituting Eq. (18) into Eq. (15) by taking account of Eq. (12) and equalizing the coefficients of $\Psi^j(\eta)$ to zero, a system of algebraic equations is acquired as follows:

$$\Psi^{-3}(\eta): \ (\beta p - 3bp - 2cp)\,B_1^3 + 6B_1 \ln(K)^2\, w^2\alpha\, p^3 = 0,$$

$$\Psi^{-2}(\eta): \ (\beta p - 3bp - 2cp)\,B_1^2 A_0 = 0,$$

$$\Psi^{-1}(\eta): \ -\frac{(-\beta + 3b + 2c)\,B_1\left(A_0^2 + A_1 B_1\right)}{p^2\alpha} + \frac{(2\alpha\, k^3 - k^2 v\lambda_2 + k^2\lambda_1 + kv - \omega)\,B_1}{p^2\left(2\alpha k - v\lambda_2 + \lambda_1\right)} - 2B_1 \ln(K)^2\, w = 0,$$

$$\Psi^0(\eta): \ \frac{\left(\frac{1}{3}\beta p - bp - \frac{2}{3}cp\right)\left(4B_1 A_0 A_1 + A_0\left(A_0^2 + 2A_1 B_1\right)\right)}{\alpha\, p^3} + \frac{(2\alpha\, k^3 - k^2 v\lambda_2 + k^2\lambda_1 + kv - \omega)\,A_0}{p^2\left(2\alpha k - v\lambda_2 + \lambda_1\right)} = 0,$$

$$\Psi(\eta): \ -\frac{(-\beta + 3b + 2c)\,A_1\left(A_0^2 + A_1 B_1\right)}{p^2\alpha} + \frac{(2\alpha\, k^3 - k^2 v\lambda_2 + k^2\lambda_1 + kv - \omega)\,A_1}{p^2\left(2\alpha k - v\lambda_2 + \lambda_1\right)} - 2A_1 \ln(K)^2\, w = 0,$$

$$\Psi^2(\eta): \ (\beta - 3b - 2c)\,A_1^2 A_0 = 0,$$

$$\Psi^3(\eta): \ (\beta - 3b - 2c)\,A_1^3 + 6A_1 p^2\alpha \ln(K)^2 = 0.$$

When this algebraic system is solved with the assistance of a Computer Algebraic Software, many solution sets are acquired. In order not to take up much volume in the article we presented some of them which we used for the graphical representations. One can also get and use other solution sets easily:

Set 1:

$$\{w = \frac{2\alpha\, k^3 - k^2 v\lambda_2 + k^2\lambda_1 + kv - \omega}{2p^2 \ln(K)^2\left(2\alpha k - v\lambda_2 + \lambda_1\right)}, A_0 = 0, A_1 = 0,$$

$$B_1 = \frac{\sqrt{6\alpha}\left(2\alpha\, k^3 - k^2 v\lambda_2 + k^2\lambda_1 + kv - \omega\right)}{2\sqrt{(-\beta + 3b + 2c)}\ln(K)\left(2\alpha k - v\lambda_2 + \lambda_1\right)p}\}. \tag{19}$$

Set 2:

$$\{w = \frac{-2\alpha\, k^3 + (v\lambda_2 - \lambda_1)\, k^2 - kv + \omega}{4\left(2\alpha k - v\lambda_2 + \lambda_1\right) p^2 \ln(K)^2},\ A_0 = 0,\ A_1 = -\frac{\sqrt{6}\,\alpha\, p \ln(K)}{\sqrt{(-\beta + 3b + 2c)}},$$

$$B_1 = -\frac{\left(3\sqrt{6}\,\sqrt{\alpha(-\beta + 3b + 2c)} + \sqrt{18\alpha b - 6\alpha\beta + 12\alpha c}\right)\left(2\alpha\, k^3 - k^2 v\lambda_2 + k^2\lambda_1 + kv - \omega\right)}{16\left(-\beta + 3b + 2c\right)\left(2\alpha k - v\lambda_2 + \lambda_1\right) p \ln(K)}\}. \tag{20}$$

Set 3:

$$\{p = \frac{\sqrt{2}\,\sqrt{w\left(2\alpha\, k^3 - k^2 v\lambda_2 + k^2\lambda_1 + kv - \omega\right)}}{2w\sqrt{\left(2\alpha k - v\lambda_2 + \lambda_1\right)}\ln(K)},\ A_0 = 0,\ A_1 = 0,$$

$$B_1 = \mp\frac{\sqrt{3w\left(-2\alpha\, k^3 + (v\lambda_2 - \lambda_1)\, k^2 - kv + \omega\right)\alpha}}{\sqrt{(-\beta + 3b + 2c)\left(-2\alpha k + v\lambda_2 - \lambda_1\right)}}\}. \tag{21}$$

Set 4:

$$\{p = \frac{\sqrt{-w\left(2\alpha\, k^3 - k^2 v\lambda_2 + k^2\lambda_1 + kv - \omega\right)}}{2w\sqrt{\left(2\alpha k - v\lambda_2 + \lambda_1\right)}\ln(K)},\ A_0 = 0,$$

$$A_1 = -\frac{\left(2\alpha\, k^3 + (-v\lambda_2 + \lambda_1)\, k^2 + kv - \omega\right)\sqrt{6}\,\alpha}{2\sqrt{-3w\left(-\frac{\beta}{3} + b + \frac{2c}{3}\right)\left(-2\alpha\, k^3 + (v\lambda_2 - \lambda_1)\, k^2 - kv + \omega\right)\left(-2\alpha k + v\lambda_2 - \lambda_1\right)\alpha}},$$

$$B_1 = -\frac{\sqrt{6}\,\sqrt{-w\left(-2\alpha\, k^3 + (v\lambda_2 - \lambda_1)\, k^2 - kv + \omega\right)\alpha}}{2\sqrt{\left(2\alpha k - v\lambda_2 + \lambda_1\right)(-\beta + 3b + 2c)}}\}. \tag{22}$$

Set 5, 6:

$$\{w = \frac{2\alpha\, k^3 + (-v\lambda_2 + \lambda_1)\, k^2 + kv - \omega}{8\left(2\alpha k - v\lambda_2 + \lambda_1\right) p^2 \ln(K)^2},\ A_0 = 0,\ A_1 = \mp\frac{\sqrt{6\alpha}\, p \ln(K)}{\sqrt{-\beta + 3b + 2c}},$$

$$B_1 = \mp\frac{\left(3\sqrt{6}\,\sqrt{\alpha(-\beta + 3b + 2c)} + \sqrt{18\alpha b - 6\alpha\beta + 12\alpha c}\right)\left(2\alpha\, k^3 - k^2 v\lambda_2 + k^2\lambda_1 + kv - \omega\right)}{16\left(-\beta + 3b + 2c\right)\left(2\alpha k - v\lambda_2 + \lambda_1\right) p \ln(K)}\}. \tag{23}$$

Accepting the $\eta_0 = 0$ and $\gamma = 1$, then substituting the functions $\Psi_i(\eta), (i = 1, 2, \ldots, 15)$ in Situation-1 to Situation-3 into Eq. (18) utilizing Eqs. (13), (16) and (17), one can acquire the solutions of Eq. (6) by substituting the Sets 1–6 above into $\vartheta_i(x, t)$. We expose the solution functions of Eq. (6), in the following general form:

$$\vartheta_1(x, t) = \left(A_0 + A_1\sqrt{w}\,\tanh_K(\xi) + \frac{B_1\,\coth_K(\xi)}{\sqrt{w}}\right)e^{i\theta}, \tag{24}$$

$$\vartheta_2(x, t) = \left(A_0 + A_1\sqrt{w}\,\coth_K(\xi) + \frac{B_1\,\tanh_K(\xi)}{\sqrt{w}}\right)e^{i\theta}, \tag{25}$$

$$\vartheta_3(x, t) = \left(A_0 + A_1\sqrt{w}\,(\tanh_K(2\xi) - i\gamma\, sech_K(2\xi)) + \frac{B_1}{\sqrt{w}(\tanh_K(2\xi) - i\gamma\, sech_K(2\xi))}\right)e^{i\theta}, \tag{26}$$

$$\vartheta_4(x, t) = \left(A_0 - \frac{A_1(w - \sqrt{w}\,\tanh_K(\xi))}{1 - \sqrt{w}\,\tanh_K(\xi)} - \frac{B_1(1 - \sqrt{w}\,\tanh_K(\xi))}{w - \sqrt{w}\,\tanh_K(\xi)}\right)e^{i\theta}, \tag{27}$$

$$\vartheta_5(x, t) = \left(A_0 - \frac{A_1\sqrt{w}(5 - 4\cosh_K(2\xi))}{3 + 4\sinh_K(2\xi)} - \frac{B_1\, 3 + 4\sinh_K(2\xi)}{\sqrt{w}(5 - 4\cosh_K(2\xi))}\right)e^{i\theta}, \tag{28}$$

$$\vartheta_6(x, t) = \left(A_0 - \frac{A_1(\gamma\sqrt{w(\rho^2 + \sigma^2)} - \rho\sqrt{w}\cosh_K(2\xi))}{\rho\sinh_K(2\xi) + \sigma} - \frac{B_1(\rho\sinh_K(2\xi) + \sigma)}{(\gamma\sqrt{w(\rho^2 + \sigma^2)} - \rho\sqrt{w}\cosh_K(2\xi))}\right)e^{i\theta}, \tag{29}$$

$$\vartheta_7(x, t) = \left(A_0 + A_1\gamma\sqrt{w}\left(1 - \frac{2\rho}{\rho + \cosh_K(2\xi) + \gamma\sinh_K(2\xi)}\right) + \frac{B_1}{\gamma\sqrt{w}\left(1 - \frac{2\rho}{\rho + \cosh_K(2\xi) + \gamma\sinh_K(2\xi)}\right)}\right)e^{i\theta}, \tag{30}$$

$$\vartheta_8(x, t) = \left(A_0 + A_1\sqrt{-w}\,\tan_K(\zeta) + \frac{B_1\,\cot_K(\zeta)}{\sqrt{-w}}\right)e^{i\theta}, \tag{31}$$

(a) 3D plot of $|\vartheta_7(x,t)|^2$

(b) contour plot of $|\vartheta_7(x,t)|^2$

(c) 2D plot of $|\vartheta_7(x,t)|^2$

(d) 2D of $|\vartheta_7(x,t)|^2$ for various c

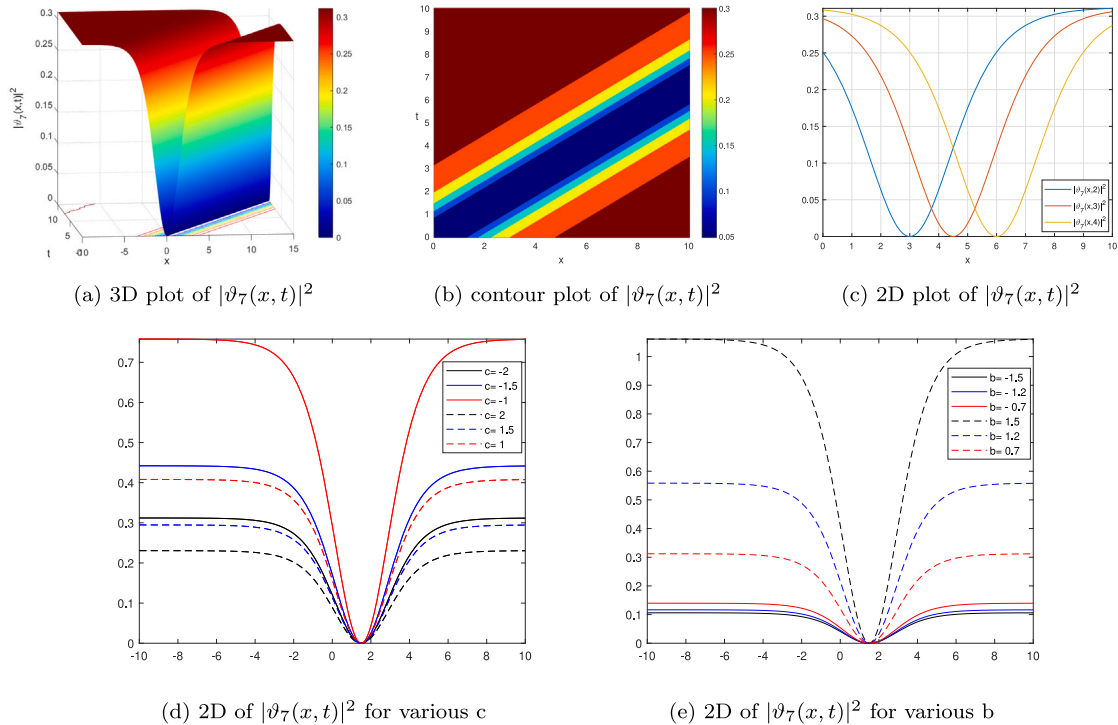(e) 2D of $|\vartheta_7(x,t)|^2$ for various b

Fig. 1. The diverse plots of $\vartheta_7(x,t)$ in Eq. (30) for the Set 1. and, the parameters $\lambda_1 = 0.5, \lambda_2 = 2, \alpha = 0.75, \beta = 1.5, b = 0.7, K = 50, \upsilon = 1.5, p = 1, \omega = 1, \varrho_0 = 10, c = -2, k = 0.75, \rho = -1$ and, $\sigma = 2$. (For interpretation of the references to color in this figure legend, the reader is referred to the web version of this article.)

$$\vartheta_9(x,t) = \left(A_0 + A_1 \sqrt{-w} \, \cot_K(\zeta) + \frac{B_1 \, \tan_K(\zeta)}{\sqrt{-w}} \right) e^{i\theta}, \tag{32}$$

$$\vartheta_{10}(x,t) = \left(A_0 - A_1 \sqrt{-w} \, (\tan_K(2\zeta) - \gamma \sec_K(2\zeta)) - \frac{B_1}{\sqrt{-w}(\tan_K(2\zeta) - \gamma \sec_K(2\zeta))} \right) e^{i\theta}, \tag{33}$$

$$\vartheta_{11}(x,t) = \left(A_0 + \frac{A_1 \sqrt{-w} \, (1 - \tan_K(\zeta))}{1 + \tan_K(\zeta)} - \frac{B_1(1 + \tan_K(\zeta))}{\sqrt{-w}\,(1 - \tan_K(\zeta))} \right) e^{i\theta}, \tag{34}$$

$$\vartheta_{12}(x,t) = \left(A_0 - \frac{A_1 \sqrt{-w}(4 - 5 \cos_K(2\zeta))}{3 + 5 \sin(2\zeta)} - \frac{B_1(5 \sin_K(2\zeta) + 3)}{\sqrt{-w}(4 - 5 \cos_K(2\zeta))} \right) e^{i\theta}, \tag{35}$$

$$\vartheta_{13}(x,t) = \left(A_0 - \frac{A_1(\gamma \sqrt{-w}(\rho^2 - \sigma^2) - \rho\sqrt{-w}\cos_K(2\zeta))}{\rho \sin_K(2\zeta) + \sigma} - \frac{B_1(\rho \sin_K(2\xi) + \sigma)}{(\gamma\sqrt{-w}(\rho^2 - \sigma^2) - \rho\sqrt{-w}\cos_K(2\zeta))} \right) e^{i\theta}, \tag{36}$$

$$\vartheta_{14}(x,t) = \left(A_0 + iA_1\gamma\sqrt{-w}\left(1 - \frac{2\rho}{\rho + \cos_K(2\zeta) + i\gamma \sin_K(2\zeta)}\right) - \frac{B_1}{\gamma\sqrt{-w}\left(1 - \frac{2\rho}{\rho + \cos_K(2\zeta) + i\gamma \sin_K(2\zeta)}\right)} \right) e^{i\theta}, \tag{37}$$

$$\vartheta_{15}(x,t) = \left(A_0 + \frac{A_1}{-kx + \omega t + \varrho_0} + B_1(-kx + \omega t + \varrho_0) \right) e^{i\theta}, \tag{38}$$

in which $\xi = \sqrt{w}(-kx + \omega t + \varrho_0)$ and $\zeta = \sqrt{-w}(-kx + \omega t + \varrho_0)$.

4. Results and discussion

In this part, we successfully carried out plethora of soliton solution for the nonlinear Schrödinger–Hirota equation in existence of perturbation terms with the effect of spatio-temporal dispersion and Kerr law nonlinearity using Mathematica, Matlab and Maple symbolic computation programs. We visualized 3D, contour and 2D plots of some solutions to present the soliton dynamic of the acquired solution with Matlab. Besides, the effect of the perturbation parameters on the solution propagation is investigated and interpreted by giving the 2D graphs obtained for different parameter values. In Fig. 1, we depict a plethora of views of $\vartheta_7(x,t)$ in Eq. (30) for the selected special parameters, which are chosen in accordance with the constraint conditions for the presence of related solutions, $\lambda_1 = 0.5, \lambda_2 = 2, \alpha = 0.75, \beta = 1.5, b = 0.7, K = 50, \upsilon = 1.5, p = 1, \omega = 1, \varrho_0 = 10, c = -2, k = 0.75, \rho = -1$ and,

(a) 3D plot of $|\vartheta_{13}(x,t)|^2$

(b) the contour plot of $|\vartheta_{13}(x,t)|^2$

(c) 2D plot of $|\vartheta_{13}(x,t)|^2$

(d) 2D of $|\vartheta_{13}(x,t)|^2$ for various c
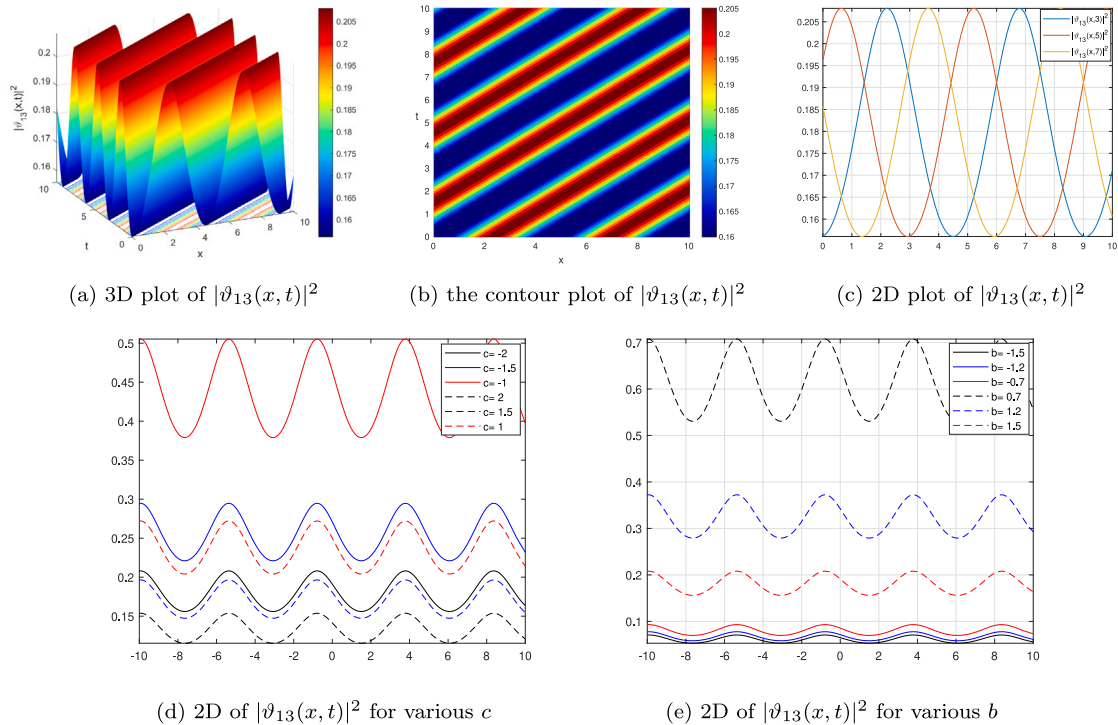
(e) 2D of $|\vartheta_{13}(x,t)|^2$ for various b

Fig. 2. The diverse plots of $\vartheta_{13}(x,t)$ in Eq. (36) for the Set 2. and, the parameters $\lambda_1 = 0.5, \lambda_2 = 2, \alpha = 0.75, \beta = 1.5, b = 0.7, K = 50, \upsilon = 1.5, p = 1, \omega = 1, \varrho_0 = 10, c = -2, k = 0.75, \rho = -1$ and, $\sigma = 2$. (For interpretation of the references to color in this figure legend, the reader is referred to the web version of this article.)

$\sigma = 2$ and in Eq. (19). Figs. 1(a), 1(b) and 1(c) represent 3D, contour and 2D plots of $|\vartheta_7(x,t)|^2$, respectively. Figs. 1(a), 1(b), 1(c) depict dark soliton solution and Fig. 1(c) also shows the traveling wave properties of the soliton, which soliton moves to the right, for $t = 2$ (blue line), $t = 3$ (red line) and $t = 4$ (yellow line). In Figs. 1(d) and 1(e), the effect of the parameters b, c which are the coefficients of self-steepening and nonlinear dispersion terms in Eq. (6) is examined while $a = 0.380$. Our main purpose is to observe how the optical soliton solution or soliton propagation behaves if these parameters change. The Fig. 1(d) shows the soliton profile of at $c = -2$ (black line), $c = -1.5$ (blue line), $c = -1$ (red line), $c = 2$ (dashed black line), $c = 1.5$ (dashed blue line) and $c = 1$ (dashed red line), respectively. We observed that, despite, there is no any movement along the x-axis, when the parameter c changes, the amplitude of $|\vartheta_7(x,1)|^2$ is changes. If $c < 0$ and c increases, the amplitude of $|\vartheta_7(x,1)|^2$ also increases. So, in this situation we can say that c has a positive correlation on the amplitude of $|\vartheta_7(x,1)|^2$. If $c > 0$ and c increases, the amplitude of $|\vartheta_7(x,1)|^2$ decreases. So, in this situation c has an inverse correlation on the amplitude of $|\vartheta_7(x,1)|^2$. The Fig. 1(e) projects the soliton profile of at $b = -1.5$ (black line), $b = -1.2$ (blue line), $b = -1$ (red line), $b = 1.5$ (dashed black line), $b = 1.2$ (dashed blue line) and $b = 0.7$ (dashed red line), respectively. Although, there is no any movement along the x-axis, when the parameter b changes, the amplitude of $|\vartheta_7(x,1)|^2$ is also changes. If $b < 0$ and b increases, the amplitude of $|\vartheta_7(x,1)|^2$ also increases. So, in this situation we can say that b has a positive correlation on the amplitude of $|\vartheta_7(x,1)|^2$. If $b > 0$ and b increases, the amplitude of $|\vartheta_7(x,1)|^2$ increases. So, b has a also positive correlation on the amplitude of $|\vartheta_7(x,1)|^2$. In case b>0 the increase in amplitude is much greater than in case b<0.

In Fig. 2, we visualize the diverse plots of the soliton solution of $\vartheta_{13}(x,t)$ in Eq. (36) for the selected special parameters, which are chosen in accordance with the constraint conditions for the existence of related solutions, $\lambda_1 = 0.5, \lambda_2 = 2, \alpha = 0.75, \beta = 1.5, b = 0.7, K = 50, \upsilon = 1.5, p = 1, \omega = 1, \varrho_0 = 10, c = -2, k = 0.75, \rho = -1$ and, $\sigma = 2$. Figs. 2(a), 2(b) and 2(c) represent 3D, contour and 2D plots of $|\vartheta_{13}(x,t)|^2$, respectively. Figs. 2(a), 2(b), 2(c) depict the periodic bright–dark soliton solution and Fig. 2(c), and also show the traveling wave properties of the soliton, which soliton moves to the right, for $t = 3$ (blue line), $t = 5$ (red line) and $t = 7$ (yellow line). In Figs. 2(d) and 2(e), our main purpose is to observe how the optical soliton solution or soliton propagation behaves if the parameters b, c parameters change while $a = 0.380$. The Fig. 2(d) shows the soliton profile of at $c = -2$ (black line), $c = -1.5$ (blue line), $c = -1$ (red line), $c = 2$ (dashed black line), $c = 1.5$ (dashed blue line) and $c = 1$ (dashed red line), respectively. We observed that, despite, there is no any movement along the x-axis as the parameter c changes, the amplitude of $|\vartheta_{13}(x,1)|^2$ is changes. As c increases for $c < 0$, the amplitude of $|\vartheta_{13}(x,1)|^2$ also increases. So, in this situation we can say that c has a positive correlation on the amplitude of $|\vartheta_{13}(x,1)|^2$. As c increases for $c > 0$, the amplitude of $|\vartheta_{13}(x,1)|^2$ decreases. So, in this situation c has a inverse correlation on the amplitude of $|\vartheta_{13}(x,1)|^2$. The Fig. 2(e) projects the soliton profile of at $b = 1.5$ (black line), $b = -1.2$ (blue line), $b = -0.7$ (red line), $b = 0.7$ (dashed black line), $b = 1.2$ (dashed blue line) and $b = 1.5$ (dashed red line), respectively. Although, there is no any movement along the x-axis as the parameter b changes, the amplitude of $|\vartheta_{13}(x,1)|^2$ is also changes. As b increases for

$b < 0$, the amplitude of $|\vartheta_{13}(x,1)|^2$ also increases. So, in this situation we can say that b has a positive correlation on the amplitude of $|\vartheta_{13}(x,1)|^2$. As b increases for $b > 0$, the amplitude of $|\vartheta_{13}(x,1)|^2$ increases. So, b has a also positive correlation on the amplitude of $|\vartheta_{13}(x,1)|^2$. In case $b > 0$ the increase in amplitude is much greater than in case $b < 0$.

In Fig. 3, we present some projections of $\vartheta_4(x,t)$ in Eq. (37) for the selected special parameters, which are chosen in accordance with the constraint conditions for the presence of related solutions, $\lambda_1 = 2, \lambda_2 = 1, \rho = -1, \sigma = 2, \alpha = 0.5, \beta = 0.8, b = 0.5, K = 10, \upsilon = 1, \omega = 1.5, \varrho_0 = 0, c = 1, k = 0.75$ and, $w = 1.5$ and in Eq. (22). Figs. 3(a), 3(b) and 3(c) represent 3D, contour and 2D plots of $|\vartheta_4(x,t)|^2$ for $t = 1$, respectively. Figs. 3(a), 3(b), and 3(c) depict the periodic bright–dark soliton solution and Fig. 3(c) also show the traveling wave properties of the soliton, which moves to the right, for $t = 1$ (blue line), $t = 3$ (red line) and $t = 5$ (yellow line). In Fig. 3(d) and e, our main purpose is to observe how the optical soliton solution or soliton propagation behaves if the parameters b, c parameters change when $a = -2.660$. The Fig. 3(d) respectively shows the soliton profile of at $c = -1.5$ (black line), $c = -1.25$ (blue line), $c = -1$ (red line), $c = 1.5$ (dashed black line), $c = 1.25$ (dashed blue line) and $c = 1$ (dashed red line). We observed that, despite, there is no any movement along the x-axis as the parameter c changes, the amplitude of $|\vartheta_4(x,1)|^2$ changes. As c increases for $c < 0$, the amplitude of $|\vartheta_4(x,1)|^2$ also increases. So, in this situation we can say that c has a positive correlation on the amplitude of $|\vartheta_4(x,1)|^2$. As c increases for $c > 0$, the amplitude of $|\vartheta_4(x,1)|^2$ decreases. So, in this situation c has a inverse correlation on the amplitude of $|\vartheta_4(x,1)|^2$. The Fig. 3(e) projects the soliton profile of at $b = -1.5$ (black line), $b = -1.25$ (blue line), $b = -1$ (red line), $b = 1.5$ (dashed black line), $b = 1.25$ (dashed blue line) and $b = 1$ (dashed red line), respectively. Although, there is no any movement along the x-axis as the parameter b changes, the amplitude of $|\vartheta_4(x,1)|^2$ is also changes. As b increases for $b < 0$, the amplitude of $|\vartheta_4(x,1)|^2$ also increases. So, in this situation we can say that b has a positive correlation on the amplitude of $|\vartheta_4(x,1)|^2$. As b increases for $b > 0$, the amplitude of $|\vartheta_4(x,1)|^2$ increases. So, b has a also positive correlation on the amplitude of $|\vartheta_4(x,1)|^2$. In case $b > 0$ the increase in amplitude is much greater than in case $b < 0$.

In Fig. 4, we illustrate some portraits of $\vartheta_{10}(x,t)$ in Eq. (33) for the selected special parameters, which are chosen in accordance with the constraint conditions for the existence of related solutions, $\lambda_1 = 0.5, \lambda_2 = 1, \alpha = 0.5, \beta = 1, b = 0.5, K = 50, \upsilon = 1, p = 1, \omega = 1.5, \varrho_0 = 10, k = 0.75, \rho = -1$ and, $\sigma = 2$. Fig. 4(a), Fig. 4(b) and Fig. 4(c) represent 3D, contour and 2D plots of $|\vartheta_{10}(x,t)|^2$ for $t = 1$, respectively. Fig. 4(a), Fig. 4(b) and Fig. 4(c) depict the bright soliton solution and, Fig. 4(c) also show the traveling wave properties of the soliton, which soliton moves to the right, for $t = 3$ (blue line), $t = 5$ (red line) and $t = 7$ (yellow line). In Figs. 4(d) and 4(e), our main purpose is to observe how the optical soliton solution or soliton propagation behaves if the parameters b, c parameters change when $a = 0.875$. The Fig. 3(d) shows the soliton profile of at $c = -1.5$ (black line), $c = -1.25$ (blue line), $c = -1$ (red line), $c = 1.5$ (dashed black line), $c = 1.25$ (dashed blue line) and $c = 1$ (dashed red line), respectively. We observed that, despite, there is no any movement along the x-axis as the parameter c changes, the amplitude of $|\vartheta_{10}(x,1)|^2$ is changes. As c increases for $c < 0$, the amplitude of $|\vartheta_{10}(x,1)|^2$ also increases. So, we can say that c has a positive correlation on the amplitude of $|\vartheta_{10}(x,1)|^2$. As c increases for $c > 0$, the amplitude of $|\vartheta_{10}(x,1)|^2$ decreases. So, in this situation c has a inverse correlation on the amplitude of $|\vartheta_{10}(x,1)|^2$. The Fig. 4(e) projects the soliton profile of at $b = -1.5$ (black line), $b = -1.25$ (blue line), $b = -0.7$ (red line), $b = 1.5$ (dashed black line), $b = 1.25$ (dashed blue line) and $b = 0.7$ (dashed red line), respectively. Although, there is no any movement along the x-axis as the parameter b changes, the amplitude of $|\vartheta_{10}(x,1)|^2$ is also changes. As b increases for $b < 0$, the amplitude of $|\vartheta_{10}(x,1)|^2$ also increases. So, in this situation we can say that b has a positive correlation on the amplitude of $|\vartheta_{10}(x,1)|^2$. As b increases for $b > 0$, the amplitude of $|\vartheta_{10}(x,1)|^2$ decreases. So, b has an inverse correlation on the amplitude of $|\vartheta_{10}(x,1)|^2$. In case $b > 0$ the increase in amplitude is much greater than in case $b < 0$.

In Fig. 5, we give a plethora of silhouettes of $\vartheta_{14}(x,t)$ in Eq. (37) for the selected special parameters, which are chosen in accordance with the constraint conditions for the presence of related solutions, $\lambda_1 = 0.8, \lambda_2 = 1, \rho = -1, \sigma = 2, \alpha = 0.75, \beta = 1, b = 1, K = 50, \upsilon = 1, \omega = 1.5, \varrho_0 = 10, c = 1, k = 0.75$ and, $w = -5$ and in Eq. (22). Figs. 5(a), 5(b) and 5(c) represent 3D, contour and 2D plots of $|\vartheta_{14}(x,t)|^2$ for $t = 1$, respectively. Figs. 5(a), 5(b), 5(c) depict the singular soliton solution and Fig. 5(c) also show the traveling wave properties of the soliton, which soliton moves to the right, for $t = 3$ (blue line), $t = 5$ (red line) and $t = 7$ (yellow line). In Fig. 5(d). and Fig. 5(e), our main purpose is to observe how the optical soliton solution or soliton propagation behaves if the parameters b, c parameters change when $a = -1.029$. The Fig. 5(d) shows the soliton profile of at $c = -0.75$ (black line), $c = -0.5$ (blue line), $c = -0.25$ (red line), $c = 0.75$ (dashed black line), $c = 0.5$ (dashed blue line) and $c = 0.25$ (dashed red line), respectively. We observed that, despite, there is no any movement along the x-axis as the parameter c changes, the amplitude of $|\vartheta_{14}(x,1)|^2$ is changes. As c increases for $c < 0$, the amplitude of $|\vartheta_{14}(x,1)|^2$ also increases. So, in this situation we can say that c has a positive correlation on the amplitude of $|\vartheta_{14}(x,1)|^2$. As c increases for $c > 0$, the amplitude of $|\vartheta_{14}(x,1)|^2$ decreases. So, in this situation c has a inverse correlation on the amplitude of $|\vartheta_{14}(x,1)|^2$. The Fig. 5(e) projects the soliton profile of at $b = -0.75$ (black line), $b = -0.5$ (blue line), $b = -0.25$ (red line), $b = 0.75$ (dashed black line), $b = 0.5$ (dashed blue line) and $b = 0.25$ (dashed red line), respectively. Although, there is no any movement along the x-axis as the parameter b changes, the amplitude of $|\vartheta_{14}(x,1)|^2$ is also changes. As b increases for $b < 0$, the amplitude of $|\vartheta_{14}(x,1)|^2$ also increases. So, in this situation we can say that b has a positive correlation on the amplitude of $|\vartheta_{14}(x,1)|^2$. As b increases for $b > 0$, the amplitude of $|\vartheta_{14}(x,1)|^2$ decreases. So, b has an inverse correlation on the amplitude of $|\vartheta_{14}(x,1)|^2$.

Last of all, we would like to emphasize that the forms of all solution functions obtained in the article with all the solution sets obtained provide the main investigated problem in Eq. (6).

5. Conclusion

In this article, we have examined a variety of solutions to the perturbed Schrödinger–Hirota equation with Kerr law non-linearity by presenting and applying the direct algebraic form of enhanced modified extended tanh expansion method. We have derived dark–bright, trigonometric, hyperbolic, periodic, and singular soliton solutions. For some values of the appropriate parameters, the 2D,
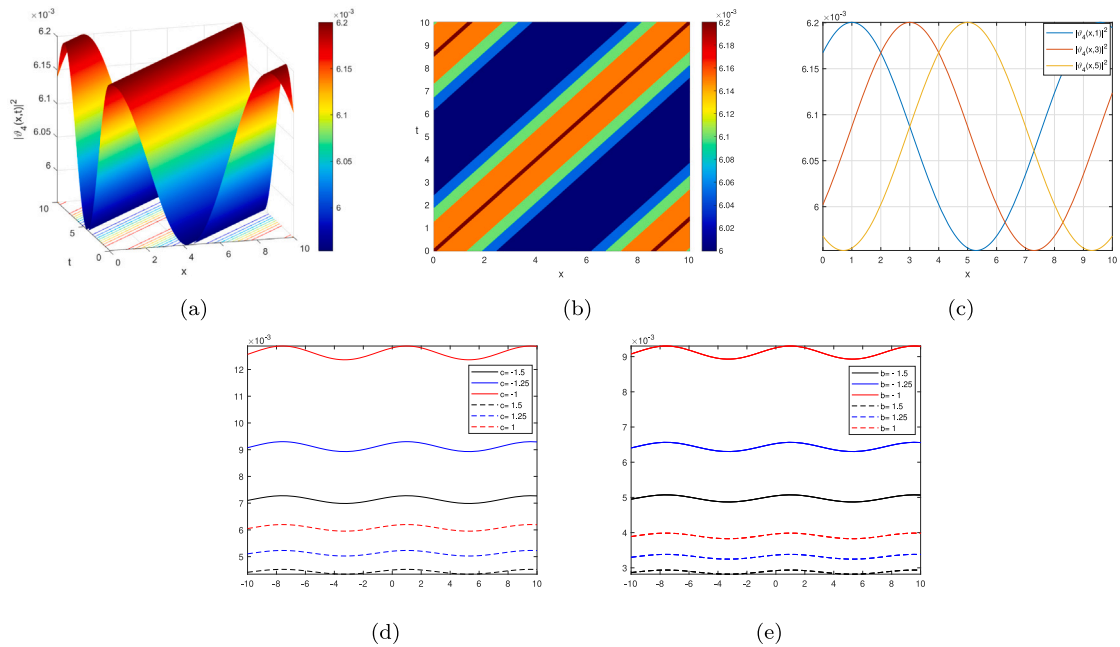
(a)

(b)

(c)

(d)

(e)

Fig. 3. The diverse plots of $|\vartheta_4(x,t)|^2$ in Eq. (27) for the Set 3 and, the parameters $\lambda_1 = 2, \lambda_2 = 1, \rho = -1, \sigma = 2, \alpha = 0.5, \beta = 0.8, b = 0.5, K = 10, \upsilon = 1, \omega = 1.5, \varrho_0 = 0, c = 1, k = 0.75$ and, $w = 1.5$. (For interpretation of the references to color in this figure legend, the reader is referred to the web version of this article.)
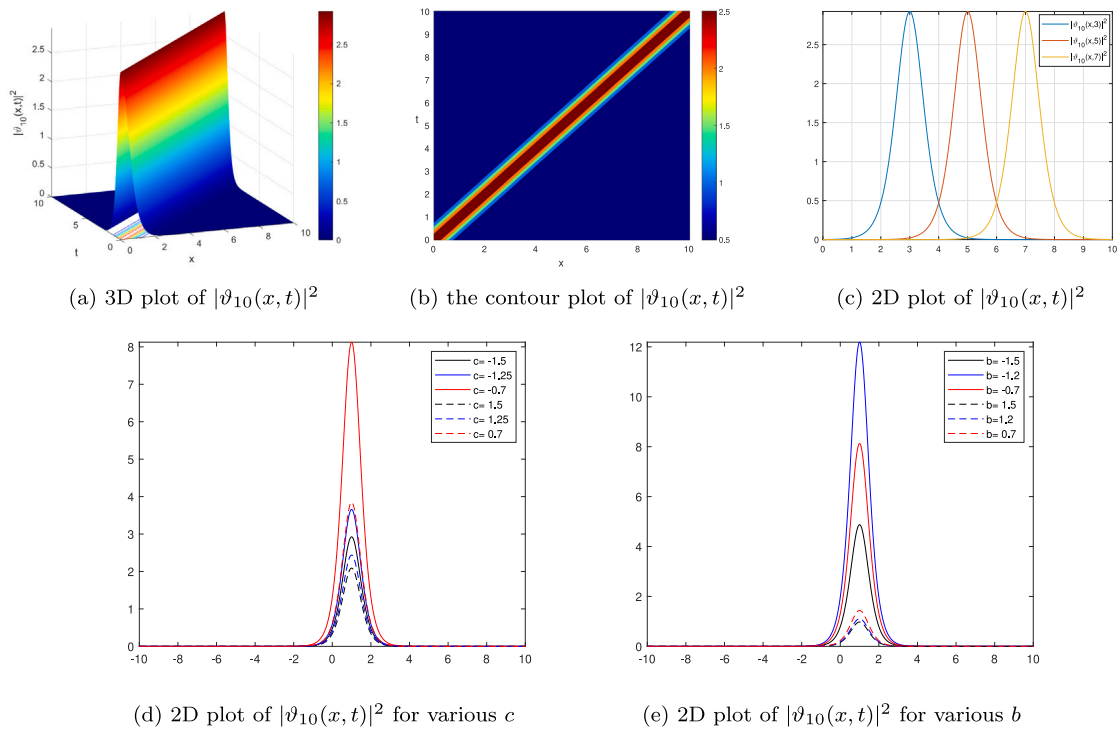

(a) 3D plot of $|\vartheta_{10}(x,t)|^2$

(b) the contour plot of $|\vartheta_{10}(x,t)|^2$

(c) 2D plot of $|\vartheta_{10}(x,t)|^2$

(d) 2D plot of $|\vartheta_{10}(x,t)|^2$ for various c

(e) 2D plot of $|\vartheta_{10}(x,t)|^2$ for various b

Fig. 4. The diverse plots of $|\vartheta_{10}(x,t)|^2$ in Eq. (33) for the Set 3. and, the parameters $\lambda_1 = 0.5, \lambda_2 = 1, \alpha = 0.5, \beta = 1, b = 0.5, K = 50, \upsilon = 1, p = 1, \omega = 1.5, \varrho_0 = 10, k = 0.75, \rho = -1$ and, $\sigma = 2$. (For interpretation of the references to color in this figure legend, the reader is referred to the web version of this article.)

contour and 3D graphs to some of the obtained solutions are illustrated. Besides, the effect of the coefficients of the self-steepening and nonlinear dispersion terms to the soliton propagation is investigated, obtained results presented graphically and interpreted in
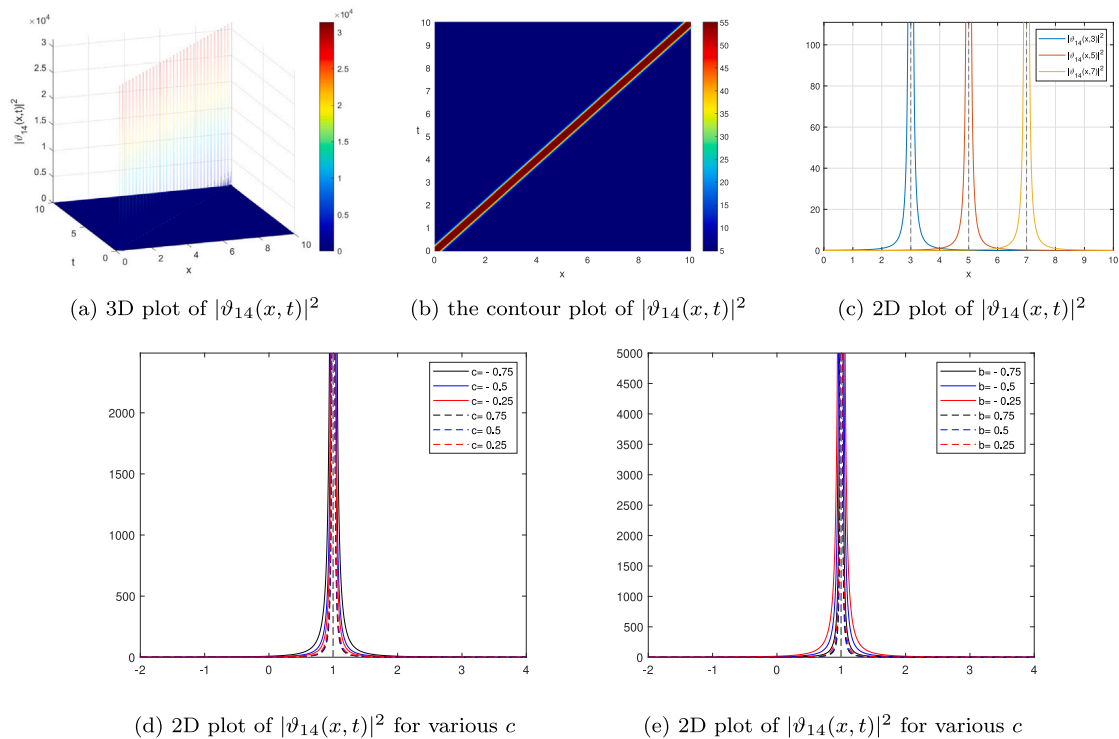
(a) 3D plot of $|\vartheta_{14}(x,t)|^2$　　　(b) the contour plot of $|\vartheta_{14}(x,t)|^2$　　　(c) 2D plot of $|\vartheta_{14}(x,t)|^2$

(d) 2D plot of $|\vartheta_{14}(x,t)|^2$ for various c　　　(e) 2D plot of $|\vartheta_{14}(x,t)|^2$ for various c

Fig. 5. The diverse plots of $|\vartheta_{14}(x,t)|^2$ in Eq. (37) for the Set 4. and, the parameters $\lambda_1 = 0.8, \lambda_2 = 1, \rho = -1, \sigma = 2, \alpha = 0.75, \beta = 1, b = 1, K = 50, \upsilon = 1, \omega = 1.5, \varrho_0 = 10, c = 1, k = 0.75$ and, $w = -5$. (For interpretation of the references to color in this figure legend, the reader is referred to the web version of this article.)

detail. The acquired results can be more helpful in interpreting the physical meaning of this nonlinear system. The proposed direct algebraic form of enhanced modified extended tanh expansion method is a powerful mathematical method which can be utilized to get the analytical solutions to a variety of the complex nonlinear mathematical models and we believe that the results obtained in the article will contribute to the studies in this field in every aspect.

Declaration of competing interest

The authors declare that they have no known competing financial interests or personal relationships that could have appeared to influence the work reported in this paper.

References

[1] A. Biswas, Quasi-stationary non-Kerr law optical solitons, Opt. Fiber Technol., Mater. Devices Syst. 9 (4) (2003) 224–259.
[2] L. Girgis, D. Milovic, S. Konar, A. Yildirim, H. Jafari, A. Biswas, Optical Gaussons in birefringent fibers and DWDM systems with intermodal dispersion, Rom. Rep. Phys. 64 (3) (2012) 663–671.
[3] H. Esen, N. Ozdemir, A. Secer, M. Bayram, Traveling wave structures of some fourth-order nonlinear partial differential equations, J. Ocean Eng. Sci. (2021).
[4] K.K. Al-Kalbani, K. Al-Ghafri, E. Krishnan, A. Biswas, Pure-cubic optical solitons by Jacobi's elliptic function approach, Optik 243 (2021) 167404.
[5] E.M. Zayed, M.E. Alngar, R.M. Shohib, A. Biswas, Y. Yıldırım, H. Triki, S.P. Moshokoa, H.M. Alshehri, Optical solitons in birefringent fibers with Sasa–Satsuma equation having multiplicative noise with Itô calculus, J. Nonlinear Opt. Phys. Mater. (2022) 2350006.
[6] S. Kumar, A. Biswas, Q. Zhou, Y. Yıldırım, H.M. Alshehri, M.R. Belic, Straddled optical solitons for cubic–quartic Lakshmanan–Porsezian–Daniel model by Lie symmetry, Phys. Lett. A 417 (2021) 127706.
[7] C.M. Khalique, A. Biswas, A Lie symmetry approach to nonlinear Schrödinger's equation with non-Kerr law nonlinearity, Commun. Nonlinear Sci. Numer. Simul. 14 (12) (2009) 4033–4040.
[8] E. Zayed, R. Shohib, M. Alngar, A. Biswas, M. Ekici, S. Khan, A. Alzahrani, M. Belic, Optical solitons and conservation laws associated with Kudryashov's sextic power-law nonlinearity of refractive index, Ukr. J. Phys. Opt. 22 (1) (2021).
[9] A. Biswas, M. Ekici, A. Sonmezoglu, Stationary optical solitons with Kudryashov's quintuple power–law of refractive index having nonlinear chromatic dispersion, Phys. Lett. A 426 (2022) 127885.
[10] M. Mirzazadeh, M. Eslami, A. Biswas, Dispersive optical solitons by Kudryashov's method, Optik 125 (23) (2014) 6874–6880.
[11] M. El-Borai, H. El-Owaidy, H.M. Ahmed, A.H. Arnous, S. Moshokoa, A. Biswas, M. Belic, Topological and singular soliton solution to Kundu–Eckhaus equation with extended Kudryashov's method, Optik 128 (2017) 57–62.
[12] A. Biswas, M. Ekici, A. Dakova, S. Khan, S.P. Moshokoa, H.M. Alshehri, M.R. Belic, Highly dispersive optical soliton perturbation with Kudryashov's sextic-power law nonlinear refractive index by semi-inverse variation, Results Phys. 27 (2021) 104539.

[13] A. Biswas, S. Arshed, Application of semi-inverse variational principle to cubic-quartic optical solitons with kerr and power law nonlinearity, Optik 172 (2018) 847–850.

[14] I. Onder, A. Secer, M. Ozisik, M. Bayram, On the optical soliton solutions of Kundu–Mukherjee–Naskar equation via two different analytical methods, Optik 257 (2022) 168761.

[15] N. Ozdemir, H. Esen, A. Secer, M. Bayram, A. Yusuf, T.A. Sulaiman, Optical soliton solutions to Chen Lee Liu model by the modified extended tanh expansion scheme, Optik 245 (2021) 167643.

[16] U. Younas, T. Sulaiman, A. Yusuf, M. Bilal, M. Younis, S. Rehman, New solitons and other solutions in saturated ferromagnetic materials modeled by Kraenkel–Manna–Merle system, Indian J. Phys. 96 (1) (2022) 181–191.

[17] G. Yel, C. Cattani, H.M. Baskonus, W. Gao, On the complex simulations with dark–bright to the Hirota–Maccari system, J. Comput. Nonlinear Dyn. 16 (6) (2021).

[18] S. Rehman, A. Yusuf, M. Bilal, U. Younas, M. Younis, T. Sulaiman, Application of (G^1/G^2)-expansion method to microstructured solids, magneto-electro-elastic circular rod and (2+ 1)-dimensional nonlinear electrical lines, Math. Eng. Sci. Aerosp. (MESA) 11 (4) (2020).

[19] S. Arshed, A. Biswas, M. Abdelaty, Q. Zhou, S.P. Moshokoa, M. Belic, Optical soliton perturbation for Gerdjikov–Ivanov equation via two analytical techniques, Chinese J. Phys. 56 (6) (2018) 2879–2886.

[20] M. Mirzazadeh, M. Eslami, B.F. Vajargah, A. Biswas, Optical solitons and optical rogons of generalized resonant dispersive nonlinear Schrödinger's equation with power law nonlinearity, Optik 125 (16) (2014) 4246–4256.

[21] G. Ebadi, A. Yildirim, A. Biswas, Chiral solitons with bohm potential using G'/G method and exp-function method, Rom. Rep. Phys. 64 (2) (2012) 357–366.

[22] S. Zhang, Exp-function method for Riccati equation and new exact solutions with two arbitrary functions of (2+ 1)-dimensional Konopelchenko–Dubrovsky equations, Appl. Math. Comput. 216 (5) (2010) 1546–1552.

[23] M. Mirzazadeh, R.T. Alqahtani, A. Biswas, Optical soliton perturbation with quadratic-cubic nonlinearity by Riccati-Bernoulli sub-ODE method and Kudryashov's scheme, Optik 145 (2017) 74–78.

[24] N. Ozdemir, H. Esen, A. Secer, M. Bayram, A. Yusuf, T.A. Sulaiman, Optical solitons and other solutions to the Hirota–Maccari system with conformable, M-truncated and beta derivatives, Modern Phys. Lett. B 36 (11) (2022) 2150625.

[25] M. Alquran, F. Yousef, F. Alquran, T.A. Sulaiman, A. Yusuf, Dual-wave solutions for the quadratic–cubic conformable-Caputo time-fractional Klein–Fock–Gordon equation, Math. Comput. Simulation 185 (2021) 62–76.

[26] M. Alquran, I. Jaradat, D. Baleanu, Shapes and dynamics of dual-mode Hirota–Satsuma coupled KdV equations: exact traveling wave solutions and analysis, Chinese J. Phys. 58 (2019) 49–56.

[27] A. Biswas, Y. Yildirim, E. Yasar, Q. Zhou, M.F. Mahmood, S.P. Moshokoa, M. Belic, Optical solitons with differential group delay for coupled Fokas–Lenells equation using two integration schemes, Optik 165 (2018) 74–86.

[28] A.J.M. Jawad, M.D. Petković, A. Biswas, Modified simple equation method for nonlinear evolution equations, Appl. Math. Comput. 217 (2) (2010) 869–877.

[29] A. Biswas, Y. Yıldırım, E. Yaşar, Q. Zhou, S.P. Moshokoa, M. Belic, Optical soliton solutions to Fokas-Lenells equation using some different methods, Optik 173 (2018) 21–31.

[30] A. Biswas, Y. Yildirim, E. Yasar, M.F. Mahmood, A.S. Alshomrani, Q. Zhou, S.P. Moshokoa, M. Belic, Optical soliton perturbation for Radhakrishnan–Kundu–Lakshmanan equation with a couple of integration schemes, Optik 163 (2018) 126–136.

[31] M.M. Al Qurashi, A.I. Aliyu, M. Inc, Optical and other solitons for the fourth-order dispersive nonlinear Schrödinger equation with dual-power law nonlinearity, Superlattices Microstruct. 105 (2017) 183–197.

[32] Y. Yan, W. Liu, Q. Zhou, A. Biswas, Dromion-like structures and periodic wave solutions for variable-coefficients complex cubic–quintic Ginzburg–Landau equation influenced by higher-order effects and nonlinear gain, Nonlinear Dynam. 99 (2) (2020) 1313–1319.

[33] A. Biswas, M. Ekici, A. Sonmezoglu, M.R. Belic, Highly dispersive optical solitons with Kerr law nonlinearity by F-expansion, Optik 181 (2019) 1028–1038.

[34] A. Biswas, M. Mirzazadeh, M. Eslami, D. Milovic, M. Belic, Solitons in optical metamaterials by functional variable method and first integral approach, Frequenz 68 (11–12) (2014) 525–530.

[35] A. Biswas, D. Milovic, R. Kohl, Optical soliton perturbation in a log-law medium with full nonlinearity by He's semi-inverse variational principle, Inverse Prob. Sci. Eng. 20 (2) (2012) 227–232.

[36] L. Akinyemi, H. Rezazadeh, Q.-H. Shi, M. Inc, M.M. Khater, H. Ahmad, A. Jhangeer, M.A. Akbar, New optical solitons of perturbed nonlinear Schrödinger–Hirota equation with spatio-temporal dispersion, Results Phys. 29 (2021) 104656.

[37] A. Biswas, Stochastic perturbation of optical solitons in Schrödinger–Hirota equation, Opt. Commun. 239 (4–6) (2004) 461–466.

[38] A. Bhrawy, A. Alshaery, E. Hilal, W.N. Manrakhan, M. Savescu, A. Biswas, Dispersive optical solitons with Schrödinger–Hirota equation, J. Nonlinear Opt. Phys. Mater. 23 (01) (2014) 1450014.

[39] J.-J. Shu, Exact N-envelope-soliton solutions of the Hirota equation, 2014, arXiv preprint arXiv:1403.3645.

[40] M. Ekici, M. Mirzazadeh, A. Sonmezoglu, M.Z. Ullah, M. Asma, Q. Zhou, S.P. Moshokoa, A. Biswas, M. Belic, Dispersive optical solitons with Schrödinger–Hirota equation by extended trial equation method, Optik 136 (2017) 451–461.

[41] A. Houwe, S. Abbagari, G. Betchewe, S.Y. Doka, K.T. Crépin, D. Baleanu, B. Almohsen, et al., Exact optical solitons of the perturbed nonlinear Schrödinger–Hirota equation with Kerr law nonlinearity in nonlinear fiber optics, Open Phys. 18 (1) (2020) 526–534.

[42] K.A. Gepreel, Exact soliton solutions for nonlinear perturbed Schrödinger equations with nonlinear optical media, Appl. Sci. 10 (24) (2020) 8929.

[43] R.A. Attia, D. Lu, T. Ak, M.M. Khater, Optical wave solutions of the higher-order nonlinear Schrödinger equation with the non-Kerr nonlinear term via modified khater method, Modern Phys. Lett. B 34 (05) (2020) 2050044.

[44] H. Bakodah, M. Banaja, A. Alshaery, A. Al Qarni, Numerical solution of dispersive optical solitons with Schrödinger-Hirota equation by improved adomian decomposition method, Math. Probl. Eng. 2019 (2019).

[45] E. Fan, Y. Hona, Generalized tanh method extended to special types of nonlinear equations, Z. Naturforsch. A 57 (8) (2002) 692–700.

[46] M. Ozisik, M. Cinar, A. Secer, M. Bayram, Optical solitons with Kudryashov's sextic power-law nonlinearity, Optik (2022) 169202.